Selection Strategy Based on Proper Pareto Optimality in Evolutionary Multi-Objective Optimization

Kai Li, Kangnian Lin, Ruihao Zheng, and Zhenkun Wang(✉)

School of System Design and Intelligent Manufacturing, Southern University of Science and Technology, Shenzhen 518055, China
Aha15380251715@gmail.com, {12132672, 12132686}@mail.sustech.edu.cn, wangzhenkun90@gmail.com

Abstract. On the multi-objective optimization problems (MOP), the dominance-resistant solution (DRS) refers to the solution that has inferior objective values but is difficult to dominate by other solutions. Prior studies have affirmed that DRSs are prevalent across MOPs and difficult to eliminate, leading to substantial performance deterioration in many multi-objective evolutionary algorithms (MOEAs). In this paper, we propose a metric inspired by proper Pareto optimality and then develop a selection strategy based on this metric (SPP) to mitigate the negative impact of DRSs. Furthermore, we implement SPP on multi-objective evolutionary algorithm based on decomposition (MOEA/D) and call the new algorithm MOEA/D-SPP. Specifically, the algorithm employs the penalty-based boundary intersection method to scalarize the MOP. Subsequently, SPP is integrated into the environmental selection. The strategy measures and sorts a set of solutions such that DRSs can be identified and removed. Finally, weight vectors are adjusted, thereby enhancing the population diversity. In experimental studies, MOEA/D-SPP outperforms five state-of-the-art MOEAs on DRS-MOPs, demonstrating the promising application of SPP.

Keywords: Multi-objective optimization · Dominance-resistant solution · Evolutionary algorithm · Proper Pareto optimality.

1 Introduction

Numerous real-world challenges, such as logistics dispatch and printed-circuit board assembly, necessitate the simultaneous consideration of multiple conflicting objectives [11,27,43]. These optimization problems are called multi-objective optimization problems (MOPs), which have the general form as follows:

$$\begin{aligned} \min. \quad & \mathbf{f}(\mathbf{x}) = (f_1(\mathbf{x}), \ldots, f_m(\mathbf{x}))^\intercal, \\ \text{s.t.} \quad & \mathbf{x} \in \Omega, \end{aligned} \tag{1}$$

where $\mathbf{x} = (x_1, \ldots, x_n)^\intercal$ represents the decision vector, also known as the solution, and $\Omega \subset \mathbb{R}^n$ signifies the feasible region. The mapping $\mathbf{f} : \mathbb{R}^n \to \mathbb{R}^m$

encompasses m objective functions, and $\mathbf{f}(\mathbf{x})$ is the objective vector corresponding to $\mathbf{x}$. Some fundamental concepts used in this paper are established below.

Definition 1. *Given two vectors $\mathbf{u}, \mathbf{v} \in \mathbb{R}^m$, $\mathbf{u}$ is said to* **dominate** *$\mathbf{v}$, iff $u_i \leq v_i$ for every $i \in \{1, \ldots, m\}$ and $u_j < v_j$ for at least one $j \in \{1, \ldots, m\}$.*

Definition 2. *A decision vector $\mathbf{x}^*$ and the corresponding objective vector $\mathbf{f}(\mathbf{x}^*)$ are* **Pareto-optimal***, if there is no $\mathbf{x} \in \Omega$ such that $\mathbf{f}(\mathbf{x})$ dominates $\mathbf{f}(\mathbf{x}^*)$.*

Definition 3. *The set of all Pareto-optimal solutions is called the* **Pareto set** *(denoted as PS), and its image in the objective space is called the* **Pareto front** *(denoted as PF).*

Definition 4 (From [13]). *A decision vector $\mathbf{x} \in \Omega$ is* **properly Pareto-optimal** *if it is Pareto-optimal and if there is some real number $M > 0$ such that for each f_i and each $\mathbf{x}'$ satisfying $f_i(\mathbf{x}') < f_i(\mathbf{x})$, there exists at least one f_j such that $f_j(\mathbf{x}) < f_j(\mathbf{x}')$ and*

$$\frac{f_i(\mathbf{x}) - f_i(\mathbf{x}')}{f_j(\mathbf{x}') - f_j(\mathbf{x})} \leq M. \tag{2}$$

Many investigations recognize the prevalence of dominance-resistant solutions (DRSs) within the feasible region of MOPs, exerting a considerable impact on the performance of various multi-objective evolutionary algorithms (MOEAs) [2,42,44]. The corresponding test problems denoted as DRS-MOPs are designed, such as mDTLZ [35] and MOP-CH [34]. A DRS has satisfactory values in at least one objective but exhibits significant deficiencies in others [18]. In other words, DRSs are close to the boundaries of the feasible objective region and remain distant from the PF. They are apart from Pareto-optimal, while few solutions can dominate them. Therefore, DRSs often persist as non-dominated solutions within the evolutionary population. For example, in Fig. 1, point B is located on the boundary parallel to the f_3 axis. Notably, B is markedly inferior to the objective vector on the PF, yet it is dominated solely by the objective vectors on line AB (i.e., red line in Fig. 1). B is recognized as dominance-resistant, due to the low possibility of discovering objective vector dominating B via evolutionary approaches. In addition, the boundary where B is situated is specifically named the hardly dominated boundary (HDB) [35]. This is because the objective vector on the HDB can improve only one objective value to obtain a better one.

Coping strategies have been developed in recent years according to the categories of MOEAs (i.e., dominance-based MOEAs [8], decomposition-based MOEAs [45], and indicator-based MOEAs [12]). Dominance-based MOEAs commonly incorporate relaxed forms of Pareto dominance [7,10,18,29,44]. Decomposition-based MOEAs utilize effective decomposition methods [14, 15, 30]. Indicator-based ones employ the environmental selection based on the hypervolume contribution [1, 12, 16]. However, the existing MOEAs encounter challenges in effectively addressing DRS-MOPs concerning convergence and diversity. In this paper, we propose a metric based on proper Pareto optimality. To test the potential of this metric, we adopt multi-objective evolutionary algorithm based on

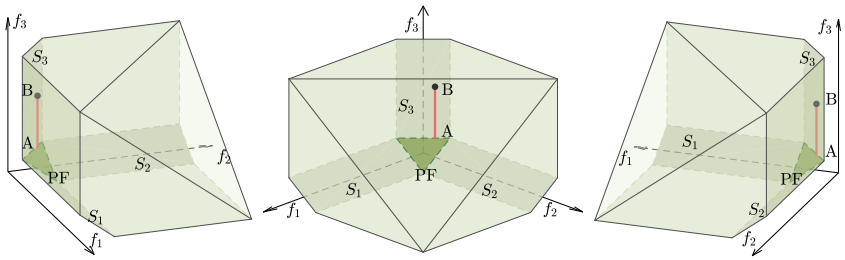

Fig. 1. Visual representations of a DRS-MOP from three distinct perspectives.

decomposition (MOEA/D) [45] as the backbone. The proposed MOEA/D variant called MOEA/D-SPP achieves competitive performance in the experiments. The contributions of this paper are encapsulated in the following:

1. The PPO metric, inspired by proper Pareto optimality, is introduced. The PPO metric of DRS is generally large. As a result, it emerges as a valuable tool for discerning DRSs effectively.
2. SPP, a selection strategy based on the PPO metric for decomposition-based MOEAs, is designed. It assesses and ranks a solution subset of the population, enabling the identification and exclusion of DRSs.
3. MOEA/D-SPP, an MOEA/D variant incorporating the newly devised selection strategy, is proposed. Additionally, a mechanism for weight vector adjustment is integrated to augment the population diversity.

The remainder of this paper is organized as follows. Section 2 introduces the motivation of this paper. Section 3 elaborates on the details of MOEA/D-SPP. Section 4 presents the numerical experiments to demonstrate the performance of MOEA/D-SPP. Finally, Section 5 concludes this paper and discusses future works.

2 Motivation

2.1 Metric Based on Proper Pareto Optimality

A solution $\mathbf{x}$ is properly Pareto-optimal when the maximum decrement among some objectives is satisfactory only at the cost of a finite increment in the others. The Definition 4 is equivalent to a properly Pareto-optimal decision vector $\mathbf{x} \in \Omega$ satisfying that:

$$h(\mathbf{x}, \mathbf{x}') = \frac{\max\limits_{1 \le i \le m} f_i(\mathbf{x}) - f_i(\mathbf{x}')}{\max\limits_{1 \le j \le m} f_j(\mathbf{x}') - f_j(\mathbf{x})} \le M < \infty, \tag{3}$$

where $\mathbf{x}' \in \Omega$ and $\max_{1 \le j \le m} f_j(\mathbf{x}') - f_j(\mathbf{x}) > 0$. We define a metric built upon $h(\mathbf{x}, \mathbf{x}')$. We refer to this metric as the PPO metric, which is formulated by:

$$\mathcal{M}_{\mathcal{S}}(\mathbf{x}) = \max_{\mathbf{x}' \in \mathcal{S}} h(\mathbf{x}, \mathbf{x}') = \max_{\mathbf{x}' \in \mathcal{S}} \left(\frac{\max\limits_{1 \le i \le m} f_i(\mathbf{x}) - f_i(\mathbf{x}')}{\max\limits_{1 \le j \le m} f_j(\mathbf{x}') - f_j(\mathbf{x})} \right), \tag{4}$$

where $\mathcal{S}$ is a solution set and $\mathbf{f}(\mathbf{x}) \neq \mathbf{f}(\mathbf{x}')$.

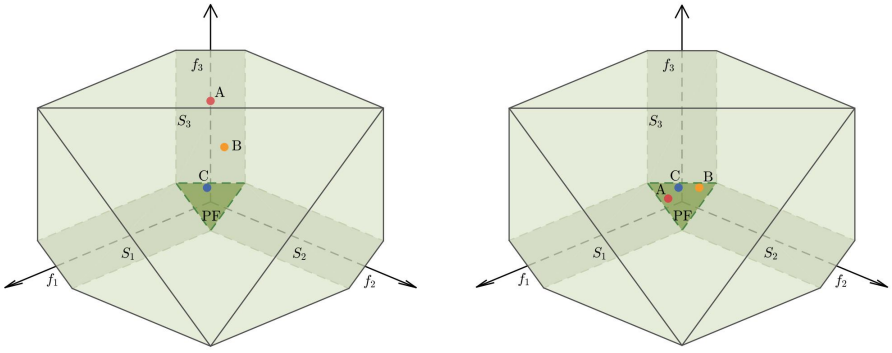

(a) Solution set with DRSs (b) Solution set without DRSs

Fig. 2. Two scenarios of the solution set $\mathcal{S}$ on a DRS-MOP.

Firstly, we examine how the PPO metric works on the solution set with DRSs. Recall that some objective values of the DRS are very poor while others are good. DRSs have a quite large value of the PPO metric. For example, Fig. 2(a) shows an example to illustrate how the PPO metric works on an MOP having DRSs. The solution set $\mathcal{S}$ is composed of three individuals A(0.25, 0.25, 1.75), B(0.25, 0.35, 1.05), and C(0.3, 0.25, 0.45), where A and B are DRSs. The PPO metric values are $\mathcal{M}_{\mathcal{S}}(\text{A}) = h(\text{A, C}) = 26$, $\mathcal{M}_{\mathcal{S}}(\text{B}) = h(\text{B, C}) = 12$, and $\mathcal{M}_{\mathcal{S}}(\text{C}) = h(\text{C, B}) \approx 0.083$, respectively. We can find that the PPO metric of DRS is larger because DRSs are extremely inferior to other solutions in some objectives.

Secondly, we investigate the solution set without DRSs. Fig. 2(b) shows an example of the solution set without DRSs. The solutions are all on the PF. The solution set $\mathcal{S}$ is composed of three individuals A(0.45, 0.25, 0.35), B(0.15, 0.4, 0.45), and C(0.3, 0.25, 0.45). The PPO metric values are $\mathcal{M}_{\mathcal{S}}(\text{A}) = h(\text{A, B}) = 2$, $\mathcal{M}_{\mathcal{S}}(\text{B}) = h(\text{B, C}) = 1$, and $\mathcal{M}_{\mathcal{S}}(\text{C}) = h(\text{C, B}) = 1$, respectively. We can find that these values are generally small. This is because the largest difference in any objective is bound by the range of the PF. We also observe that these objective vectors have different PPO metric values. The calculation of the metric is based on the difference in the objectives, and thus different distributions of solutions can lead to distinct metric values. In other words, the distances between solutions and the density of solutions can affect the PPO metric values.

In short, The PPO metric is a potential criterion for identifying DRSs. When $\mathcal{M}_{\mathcal{S}}(\mathbf{x})$ is quite large, $\mathbf{x}$ strikes a poor trade-off between some objectives. We can remove DRSs by removing the solutions that have large PPO metric values. Moreover, an additional scheme for the PPO metric is required to avoid accidentally eliminating a good solution.

2.2 MOEA/D

MOEA/D uses weight vectors and scalarization methods to convert an MOP into many single-objective optimization subproblems and solves these subproblems collaboratively. The effectiveness of MOEA/D is demonstrated in addressing various MOPs [36–38]. The performance of MOEA/D highly depends on the scalarization methods, and different scenarios may require different scalarization methods [19, 46]. However, only some existing scalarization methods can cope with DRSs. For example, the penalty boundary intersection (PBI) method [45] fails as found in [34]. We suggest employing the PPO metric, which enables the application of any scalarization method in scenarios involving DRSs. $\mathcal{S}$ in the PPO metric is specified as $\mathcal{S}_i$ containing several closest solutions to the i-th subproblem and the offspring o_i. Thereafter, the DRSs with respect to the i-th subproblem can be distinguished.

In the following section, we propose MOEA/D-SPP, which selects solutions based on the PPO metric. The PBI method is used in MOEA/D-SPP. Let $\mathbf{w}$ be a weight vector and $\mathbf{z}^*$ be the ideal point, and the mathematical expression defining the PBI-based subproblem is as follows:

$$\text{min.} \quad g^{\text{pbi}}(\mathbf{x}|\mathbf{w}, \mathbf{z}^*) = d_1 + \theta d_2, \tag{5}$$

where

$$\begin{aligned} d_1 &= \frac{|(\mathbf{f}(\mathbf{x}) - \mathbf{z}^*)^\mathsf{T} \mathbf{w}|}{\|\mathbf{w}\|_2} \ , \\ d_2 &= \left\| \mathbf{f}(\mathbf{x}) - \mathbf{z}^* - d_1 \frac{\mathbf{w}}{\|\mathbf{w}\|_2} \right\|_2 \ . \end{aligned} \tag{6}$$

θ is a penalty parameter and we adopt $\theta = 10$ in this paper. Additionally, DRS-MOPs are often characterized by irregular PFs, while the performance of MOEA/D is also influenced by the shape of the PF [20, 35, 40, 41]. Therefore, when applying MOEA/D to address DRS-MOPs, adjusting the weight vectors is also important to enhance its performance.

3 Algorithm

3.1 Framework

The framework of MOEA/D-SPP is outlined in Algorithm 1. The two key algorithmic components, namely **IdentifyDRS** and **AdjustWeights**, are detailed

in Algorithm 2 and Algorithm 3, respectively. **IdentifyDRS** is the selection strategy based on the PPO metric. **AdjustWeights** can adjust weight vectors properly. We adopt a multistage procedure [9]: the first stage is the same as MOEA/D-PBI; **IdentifyDRS** is introduced in the second stage; **IdentifyDRS** still executes and **AdjustWeights** improves the diversity finally.

Algorithm 1 MOEA/D-SPP

Input: N (population size); G_{max} (maximum number of generations); T (neighborhood size); ϑ_{stage}, and a (control parameters).
Output: $\mathcal{P}$ (the final population).

1: Generate a random population $\mathcal{P} = \{\mathbf{x}_1, \ldots, \mathbf{x}_N\}$;
2: Generate the set of weight vectors $\mathcal{W} = \{\mathbf{w}_1, \ldots, \mathbf{w}_N\}$, and assign T neighboring subproblems for each subproblem (denote the neighborhood of the i-th subproblem as $\mathcal{B}_i$);
3: Set $isUsed \leftarrow false$;
4: **for** $gen = 1$ to G_{max} **do**
5: **for** each subproblem $(i = 1, \ldots, N)$ **do**
6: Select solutions from $\mathcal{B}_i$ to generate the offspring $\mathbf{o}_i$;
7: **if** $gen > \vartheta_{stage}$ **then**
8: ($\mathcal{P}$, $flag$) $\leftarrow$ **IdentifyDRS** ($\mathcal{P}$, $\mathbf{o}_i$, T, a);
9: **if** $flag = false$ **then**
10: **Continue**;
11: **end if**
12: **end if**
13: Update the $\mathcal{B}_i$ with $\mathbf{o}_i$;
14: **end for**
15: **if** $gen > 2 \cdot \vartheta_{stage}$ and $isUsed = false$ **then**
16: $\mathcal{W} \leftarrow$ **AdjustWeights** ($\mathcal{P}$);
17: $isUsed \leftarrow true$;
18: **end if**
19: **end for**

The algorithm first initiates the population $\mathcal{P}$ and the set of weight vectors $\mathcal{W}$ and determines neighbors for each weight vector (lines 1-2). The neighborhood of the i-th subproblem is denoted as $\mathcal{B}_i$. Subsequently, $isUsed$ is introduced, which represents the evolutionary stage. In MOEA/D-SPP, different goals are achieved at different stages. It is set to 0 initially (line 3). After the initialization, the algorithm iterates over each subproblem. For the subproblem with index i in each generation (line 5), the algorithm first selects solutions from $\mathcal{B}_i$ to generate the offspring $\mathbf{o}_i$ (line 6). Subsequently, if the generation number gen surpasses the control parameter ϑ_{stage}, the **IdentifyDRS** component is executed. This component employs the PPO metric to identify DRSs (lines 7-8). If the offspring $\mathbf{o}_i$ is considered to be a DRS (i.e., $flag = false$), the algorithm skips updating $\mathcal{B}_i$ with $\mathbf{o}_i$ and proceeds to the next subproblem (lines 9-11). Otherwise, $\mathbf{o}_i$ is used to update $\mathcal{B}_i$ according to the PBI method (line 13). If $gen \leq \vartheta_{stage}$, the **IdentifyDRS** component remains inactive and the subproblem is updated

regularly. Moreover, if gen surpasses $2 \cdot \vartheta_{stage}$ and $isUsed = false$ (line 15), the **AdjustWeights** component is invoked only once. The weight vectors are adjusted to the appropriate distribution according to the current population, thereby enhancing the population diversity in subsequent iterations (line 16). It indicates **AdjustWeights** is used and let $isUsed$ be $true$ (line 17). Finally, the population $\mathcal{P}$ is returned as the output of the algorithm.

3.2 Selection Strategy Based on PPO Metric (SPP)

The **IdentifyDRS** component, as illustrated in Algorithm 2, plays a crucial role within the MOEA/D-SPP framework. It employs the PPO metric to assess the acceptance of new solutions and the removal of old ones, which can effectively distinguish the DRSs.

Algorithm 2 IdentifyDRS $(\mathcal{P}, \mathbf{o}_i, T, a)$

Input: $\mathcal{P}$ (the population); $\mathbf{o}_i$ (the offspring); T (the neighborhood size) and a (control parameter).

Output: $\mathcal{P}$ (the updated population); $flag$ (the symbol indicating whether to accept the offspring).

1: $\mathcal{S}_i \leftarrow \{T$ solutions closest to $\mathbf{w}_i$, $\mathbf{o}_i\}$;
2: Compute the PPO metric for each solution in P_i according to Eq. (4);
3: $\mathbf{x}_{worst} \leftarrow \arg\max_{\mathbf{x} \in \mathcal{S}_i} \{\mathcal{M}_{\mathcal{S}_i}(\mathbf{x})\}$;
4: **if** $\mathbf{o}_i$ is $\mathbf{x}_{worst}$ or $\mathcal{M}_{\mathcal{S}_i}(o_i) \geq a$ **then**
5: $\quad flag \leftarrow false$;
6: $\quad$ **return**;
7: **else**
8: $\quad flag \leftarrow true$;
9: **end if**
10: **if** $\mathcal{M}_{\mathcal{S}_i}(\mathbf{x}_{worst}) \geq N^{1/(m-1)}$ **then**
11: $\quad$ **repeat**
12: $\quad\quad \mathbf{x}' \leftarrow$ Randomly select from $\mathcal{S}_i$;
13: $\quad$ **until** $\mathcal{M}_{\mathcal{S}_i}(\mathbf{x}') \leq a$ or $\mathbf{x}' = \arg\min_{\mathbf{x} \in \mathcal{S}_i} \{\mathcal{M}_{\mathcal{S}_i}(\mathbf{x})\}$
14: $\quad$ Replace the solution in P corresponding to $\mathbf{x}_{worst}$ with $\mathbf{x}'$;
15: **end if**

The algorithmic component initiates by constructing a set $\mathcal{S}_i$ comprising the T solutions closest to the weight vector $\mathbf{w}_i$ and the offspring $\mathbf{o}_i$ (line 1). For each solution in $\mathcal{S}_i$, the PPO metric is computed according to Eq. (4) (line 2). The solution with the worst PPO metric value, denoted as $\mathbf{x}_{worst}$, is identified (line 3). Thereafter, the algorithm checks whether the current offspring $\mathbf{o}_i$ is $\mathbf{x}_{worst}$ or if its PPO metric value exceeds the predefined value a (line 4). If either condition is met, the offspring is deemed to have poor quality. Then the offspring should not be accepted and the algorithm returns $flag$ of $false$ and the unchanged $\mathcal{P}$ (lines 5-6). Otherwise, the offspring is considered suitable to be accepted and let $flag$ be $true$ (line 8).

As mentioned in Section 2.1, the PPO metric values of the solutions on the PF are related to the population density. The density of uniform sampling points suffers from the curse of dimensionality and the density is proportional to $q^{1/p}$, where p is the space dimension and q is the sample size [3,17]. We adopt the threshold of $N^{1/(m-1)}$ considering that the PF is an $(m-1)$ dimensional manifold. Specifically, when the PPO metric of $\mathbf{x}_{worst}$ exceeds $N^{1/(m-1)}$ (line 10), the algorithm substitutes the solution in P that corresponds to $\mathbf{x}_{worst}$ by randomly selecting a suitable solution from $\mathcal{S}_i$ (lines 11-14).

3.3 Adjustment of Weight Vectors

The **AdjustWeights** component, shown in Algorithm 3, aims to improve the diversity of the population. It generates a set of new weight vectors based on the distribution of solutions in the current population.

Algorithm 3 AdjustWeights ($\mathcal{P}$)

Input: $\mathcal{P}$ (the population).
Output: $\mathcal{W}$ (the set of weight vectors).
1: $p \leftarrow$ Estimate a parameter via $\mathcal{P}$ for the PF shape [24];
2: $\mathcal{R} \leftarrow$ Generate a set of uniformly distributed weight vectors;
3: $w_i \leftarrow 1 - w_i^{1/p}$ for $i = 1, \ldots, m$ and every $\mathbf{w} \in \mathcal{R}$;
4: $\mathcal{W} \leftarrow \emptyset$;
5: **for** $i = 1$ to m **do**
6: $\quad \mathbf{w}_{tmp} \leftarrow \arg\min_{\mathbf{w} \in \mathcal{R}} w_i$;
7: $\quad \mathcal{W} \leftarrow \mathcal{W} \cup \mathbf{w}_{tmp}$;
8: $\quad \mathcal{R} \leftarrow \mathcal{R} \setminus \mathbf{w}_{tmp}$;
9: **end for**
10: **while** $|\mathcal{W}| < N$ **do**
11: $\quad \mathbf{w}_{tmp} \leftarrow \arg\max_{\mathbf{w} \in \mathcal{R}} \left\{ \min_{\mathbf{v} \in \mathcal{W}} ||\mathbf{w} - \mathbf{v}||_2 \right\}$;
12: $\quad \mathcal{W} \leftarrow \mathcal{W} \cup \mathbf{w}_{tmp}$;
13: $\quad \mathcal{R} \leftarrow \mathcal{R} \setminus \mathbf{w}_{tmp}$;
14: **end while**

To estimate the shape of the PF, the component is inspired by [24] to estimate the PF shape by finding the most consistent contour curve of the modified L_p-norm distance (line 1). This estimation works as follows:

1. Firstly, compute the modified L_p-norm distances for objective vectors of $\mathcal{P}$ using candidate values of p ($p > 0$). The set of distances is denoted as $G_p = \{g(\mathbf{x}|p) \mid \mathbf{x} \in \mathcal{P}\}$ where $g(\mathbf{x}|p) = \left(\sum_{i=1}^{m}(1 - f_i(\mathbf{x}))^p\right)^{1/p}$.
2. Secondly, select the p value with smallest standard deviation of G_p.

In other words, the estimation determines a value of p.

After that, a sufficiently large set of uniformly distributed weight vectors $\mathcal{R}$ is generated by using the two-layer weight vectors generation method [6,23] (line

2). The endpoints of weight vectors in $\mathcal{R}$ are located on the unit simplex. With p and $\mathcal{R}$, the desired weight vectors can be obtained. Each $\mathbf{w} \in \mathcal{R}$ is transformed based on the value of p (line 3). The transformation method is consistent with the aforementioned estimation method. Then, a subset $\mathcal{W}$ is selected from $\mathcal{R}$. The component finds m extreme weight vectors as initialized elements in $\mathcal{W}$ (lines 5-8). In line 6, we can find that the extreme weight vectors represent those having the lowest value on at least one objective. The remaining $(N-m)$ weight vectors for $\mathcal{W}$ are chosen from $\mathcal{R}$ one by one (lines 10-14). Sparse weight vectors are prioritized for selection. The sparsity of a weight vector is defined in line 11. In other words, the sparsity is the minimum Euclidean distance from the weight vector to the one within $\mathcal{W}$.

4 Numerical Experiments

4.1 Benchmark Problems

In this section, we assess the proposed MOEA/D-SPP on mDTLZ1-mDTLZ4 [35]. These test problems exhibit two common features: 1) irregularity in the PF shape (e.g., the PF of mDTLZ1 is an inverted triangle); and 2) complexity in the feasible objective region (e.g., all problems exhibit HDBs). Note that an MOP featuring more than 3 objectives is viewed as a many-objective optimization problem. We consider 3 and 5 as two settings of the objective dimension. The number of decision variables is set to 10 for 3-objective problems and 12 for 5-objective problems in each instance.

Each algorithm undergoes 30 independent runs on each test instance. The population size is set to 105 for 3-objective instances and 210 for the 5-objective instances. The maximum number of function evaluations is set to 105,000 (i.e., 105×1000) for the 3-objective case and 252,000 (i.e., 210×1200) for the 5-objective case. All experiments are conducted on the PlatEMO platform [32].

4.2 Evaluation Metrics

The inverted generational distance (IGD) metric [4] and the hypervolume (HV) metric [47] are employed for assessing the performance of the obtained solution sets. IGD calculates the average distances from each objective vector to its nearest reference point of the PF. A smaller IGD value indicates a better performance of the algorithm. HV describes the size of the region covered by the obtained objective vectors and the reference point. A larger HV value represents the better performance of the algorithm.

The mean metric values are employed to show the statistical performance of each algorithm on each test problem [22, 26, 39]. Statistical analysis of the differences between mean metric values is conducted using Wilcoxon's rank-sum test at a significance level of 0.05 [21]. The symbols "+", "−", and "=" denote that the compared algorithm performs statistically better than, worse than, and equal to MOEA/D-SPP, respectively.

4.3 Compared Algorithms

We conduct a comparative analysis of our proposed algorithm against five representative MOEAs. The parameters of algorithms are configed according to the corresponding references. NSGA-II [8] is a classical dominance-based MOEA utilizing the Pareto dominance criterion and employing crowding distance for diversity evaluation. MOEA/D-Gen [15] utilizes generalized decomposition, with parameters δ and ρ set to 0.01. mNSGA-II [31] addresses DRSs by modifying objective values, with control parameter α set to 0.01. PMEA [28] incorporates preprocessing and penalty mechanisms, with parameter r set to 1.5. MOEA/D-OMDEA [33] integrates the OM-dominance criterion, with parameters $\alpha_1 = 0.25$, $\alpha_2 = 0.1$, $\tau = 0.7$, and $K = 30$ for 3-objective cases and $K = 50$ for 5-objective cases.

In our compared algorithms, the control parameters in MOEA/D-SPP are established as $a = 2$ and $\vartheta_{stage} = 300$. In general, the neighborhood size T for MOEA/D variants is set to $\lceil N/10 \rceil$. All the algorithms except for MOEA/D-OMDEA employ the simulated binary crossover and polynomial mutation [5] to generate new solutions. The distribution indexes are set to 20. Besides, the crossover and mutation probabilities are configured at 1 and $1/n$ respectively. MOEA/D-OMDEA follows the operators outlined in [25].

4.4 Comparison Results

The mean IGD and HV metric values achieved by algorithms on all instances are presented in Table 1 and 2 respectively. The best result for each problem is highlighted in bold. the standard deviations of means are in parentheses.

In Table 1, MOEA/D-SPP exhibits the best mean IGD metric values on 3-objective mDTLZ1, mDTLZ2, and mDTLZ3. Furthermore, according to Wilcoxon's rank-sum test, MOEA/D-SPP outperforms NSGA-II, MOEA/D-Gen, mNSGA-II, PMEA, and MOEA/D-OMDEA on 7, 5, 6, 6, and 6 out of 8 instances, respectively. In contrast, it is significantly outperformed by NSGA-II, MOEA/D-Gen, and MOEA/D-OMDEA on 1, 2, and 1 out of 8 problems. In summary, MOEA/D-SPP demonstrates a substantial improvement in terms of the IGD metric compared to these competitors.

In Table 2, the best HV result of each instance is achieved by the following algorithms: MOEA/D-SPP on mDTLZ1-mDTLZ3 and PMEA on mDTLZ4. According to Wilcoxon's rank-sum test, MOEA/D-SPP outperforms NSGA-II, MOEA/D-Gen, mNSGA-II, PMEA, and MOEA/D-OMDEA on 8, 7, 7, 6, and 7 out of 8 instances, respectively. It is only outperformed by mNSGA-II, PMEA, and MOEA/D-OMDEA on 1, 2, and 1 out of 8 instances. Overall, MOEA/D-SPP also demonstrates advantages over these peer algorithms in terms of the HV metric.

The overall result of the IGD metric conforms to that of the HV metric. The proposed MOEA/D-SPP exhibits competitive performance with respect to both IGD and HV metrics on 3-objective and 5-objective mDTLZ1-mDTLZ4. Furthermore, Friedman tests are conducted to compare MOEA/D-SPP with

Table 1. Means and standard deviations of IGD metric values obtained by algorithms.

IGD	m	NSGA-II	MOEA/D-Gen	mNSGA-II	PMEA	MOEA/D-OMDEA	MOEA/D-SPP
mDTLZ1	3	1.0787e+0 - (1.35e+0)	2.9330e-2 - (4.38e-5)	2.6286e-2 - (1.66e-3)	3.1430e-2 - (1.37e-3)	1.7657e-1 - (1.04e-1)	**2.1800e-2** (1.06e-2)
mDTLZ2	3	1.1600e-1 - (8.91e-3)	6.9634e-2 - (2.69e-4)	6.3331e-2 - (2.01e-3)	1.0411e-1 - (2.18e-2)	7.6944e-2 - (9.40e-3)	**5.4112e-2** (9.91e-4)
mDTLZ3	3	2.0386e+0 - (2.67e+0)	6.9580e-2 - (3.35e-4)	6.4027e-2 - (4.02e-3)	9.8289e-2 - (1.47e-2)	1.2934e-1 - (5.10e-2)	**5.8790e-2** (4.06e-3)
mDTLZ4	3	1.3340e-1 - (1.26e-2)	1.1960e-1 - (1.17e-1)	8.0513e-2 = (1.56e-2)	7.9877e-2 = (1.05e-2)	**7.7648e-2** = (4.84e-3)	1.1494e-1 (1.71e-1)
mDTLZ1	5	2.8688e+1 - (1.63e+1)	5.7983e-2 - (2.61e-5)	1.5148e-1 - (1.91e-2)	9.6846e-2 - (6.68e-3)	2.7975e-1 - (8.98e-2)	**5.6686e-2** (3.45e-3)
mDTLZ2	5	2.4618e-1 - (1.52e-2)	**1.4887e-1** + (5.02e-4)	2.1538e-1 - (9.02e-3)	2.8372e-1 - (2.84e-2)	1.8211e-1 + (1.12e-2)	1.9844e-1 (2.47e-2)
mDTLZ3	5	4.7116e+1 - (3.55e+1)	**1.4780e-1** + (9.80e-4)	3.9344e-1 - (2.75e-2)	3.1063e-1 - (3.63e-2)	4.4687e-1 - (1.21e-1)	2.1978e-1 (3.01e-2)
mDTLZ4	5	2.8455e-1 + (1.69e-2)	2.1408e-1 = (4.45e-2)	2.2922e-1 = (1.61e-2)	**2.1218e-1** = (1.78e-2)	3.3439e-1 - (3.08e-2)	3.0939e-1 (2.05e-1)
+/-/=		1/7/0	2/5/1	0/6/2	0/6/2	1/6/1	–

Table 2. Means and standard deviations of HV metric values obtained by algorithms.

HV	m	NSGA-II	MOEA/D-Gen	mNSGA-II	PMEA	MOEA/D-OMDEA	MOEA/D-SPP
mDTLZ1	3	2.8699e-2 - (2.79e-2)	5.1641e-1 - (4.89e-4)	5.0487e-1 - (5.16e-3)	4.7351e-1 - (7.56e-3)	1.8425e-1 - (1.46e-1)	**5.2067e-1** (3.01e-2)
mDTLZ2	3	8.6691e-1 - (2.51e-2)	1.0237e+0 - (1.35e-4)	1.0207e+0 - (4.13e-3)	1.0152e+0 - (9.03e-3)	1.0011e+0 - (7.03e-3)	**1.0340e+0** (1.16e-3)
mDTLZ3	3	3.5195e-2 - (4.30e-2)	1.0234e+0 - (5.67e-4)	1.0227e+0 - (6.07e-3)	9.9438e-1 - (1.06e-2)	8.4447e-1 - (1.26e-1)	**1.0314e+0** (4.75e-3)
mDTLZ4	3	7.9821e-1 - (3.41e-2)	8.7509e-1 - (1.38e-1)	9.5801e-1 + (5.06e-2)	**9.9996e-1** + (4.33e-2)	9.7326e-1 + (7.34e-3)	8.8277e-1 (1.83e-1)
mDTLZ1	5	2.6754e-5 - (1.47e-4)	6.6176e-2 - (3.26e-4)	1.2345e-2 - (3.16e-3)	2.4288e-2 - (3.63e-3)	1.7688e-3 - (2.09e-3)	**7.7432e-2** (6.42e-3)
mDTLZ2	5	1.8242e-1 - (2.20e-2)	3.9667e-1 - (1.50e-3)	2.6287e-1 - (1.41e-2)	4.4651e-1 - (4.40e-3)	4.0032e-1 - (6.41e-3)	**4.6319e-1** (2.30e-3)
mDTLZ3	5	0.0000e+0 - (0.00e+0)	4.0003e-1 - (1.87e-3)	3.3793e-2 - (1.70e-2)	2.8197e-1 - (1.41e-2)	8.9890e-2 - (7.18e-2)	**4.6964e-1** (3.11e-3)
mDTLZ4	5	1.3682e-1 - (1.55e-2)	3.0907e-1 = (6.46e-2)	2.0975e-1 - (2.81e-2)	**4.3240e-1** + (4.44e-3)	1.1367e-1 - (3.24e-2)	3.0900e-1 (1.30e-1)
+/-/=		0/8/0	0/7/1	1/7/0	2/6/0	1/7/0	–

Table 3. Average ranks of representative algorithms and MOEA/D-SPP obtained by Friedman test.

	IGD	HV
NSGA-II	5.625	5.875
MOEA/D-Gen	2.5	2.625
mNSGA-II	3	3.75
PMEA	3.5	2.75
MOEA/D-OMDEA	4.125	4.375
MOEA/D-SPP	**2.25**	**1.625**

five other algorithms. Table 3 reveals that MOEA/D-SPP achieves the best average rankings across both metrics, signifying its superior performance over

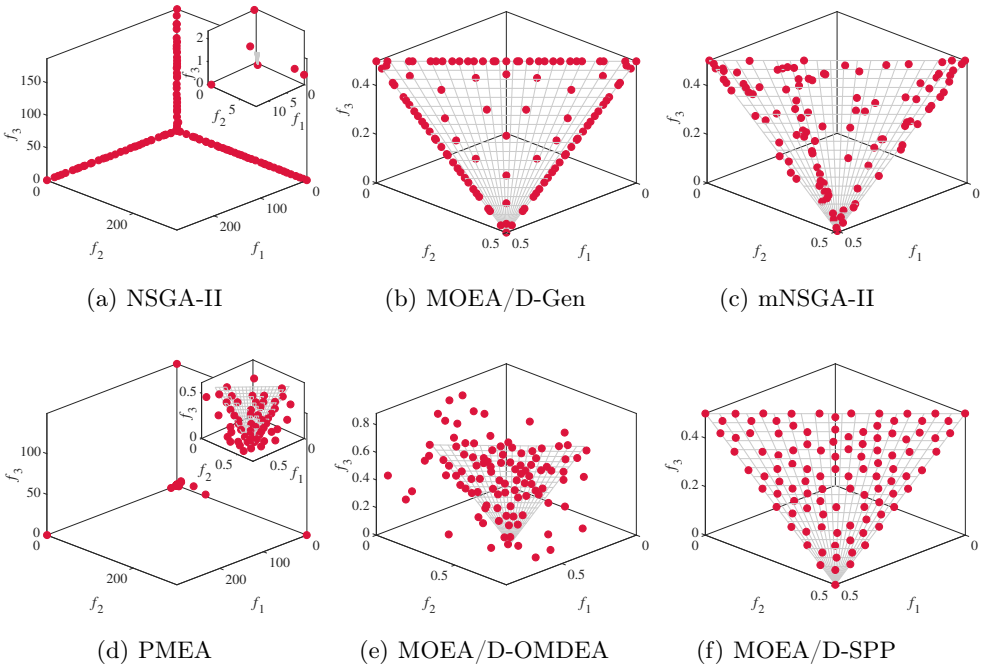

(a) NSGA-II (b) MOEA/D-Gen (c) mNSGA-II

(d) PMEA (e) MOEA/D-OMDEA (f) MOEA/D-SPP

Fig. 3. The approximate set with the median IGD metric value on 3-objective mDTLZ1.

the other algorithms. We visualize the approximate set of each algorithm on 3-objective mDTLZ1 in Fig. 3. The approximate set with the median IGD metric value among 30 runs is selected. These figures reveal that only MOEA/D-SPP discovers a well-distributed solution set across the entire PF, effectively balancing the convergence and diversity.

4.5 Effectiveness Analysis

The proposed MOEA/D-SPP utilizes the PBI method and introduces two key algorithmic components: **IdentifyDRS** and **AdjustWeights**. To investigate the individual effectiveness of each component within the proposed algorithm, several ablation experiments are conducted. MOEA/D-SPP is compared with the following three variants:

- V-a: MOEA/D-SPP without the execution of any of the two components. In such a case, its behavior is identical to that of MOEA/D-PBI.
- V-b: MOEA/D-SPP without **AdjustWeights**.
- V-c: MOEA/D-SPP without **IdentifyDRS**.

Experimental results are presented in Table 4 and Table 5. The results show that MOEA/D-SPP outperforms other variants of MOEA/D-SPP in terms of

Table 4. Means and standard deviations of IGD metric values obtained by MOEA/D-SPP and its variants.

IGD	m	V-a	V-b	V-c	MOEA/D-SPP
mDTLZ1	3	4.5380e-2 - (4.19e-3)	3.0038e-2 - (3.72e-4)	9.3394e-2 - (4.27e-2)	**2.1800e-2** (1.06e-2)
mDTLZ2	3	7.3003e-2 - (7.08e-4)	7.8833e-2 - (4.13e-3)	7.5943e-2 - (1.41e-3)	**5.4112e-2** (9.91e-4)
mDTLZ3	3	7.3931e-2 - (1.35e-3)	1.0710e-1 - (9.50e-3)	9.7051e-2 - (4.08e-2)	**5.8790e-2** (4.06e-3)
mDTLZ4	3	1.8893e-1 - (1.72e-1)	1.5781e-1 - (1.56e-1)	2.1567e-1 - (2.21e-1)	**1.1494e-1** (1.71e-1)
mDTLZ1	5	1.7306e-1 - (1.12e-3)	8.4131e-2 - (5.13e-3)	1.0720e-1 - (5.07e-3)	**5.6686e-2** (3.45e-3)
mDTLZ2	5	3.3092e-1 - (3.07e-3)	3.2329e-1 - (1.80e-2)	**1.5836e-1** + (6.90e-3)	1.9844e-1 (2.47e-2)
mDTLZ3	5	3.0808e-1 - (1.91e-3)	3.2506e-1 - (2.00e-2)	**2.1385e-1** = (1.70e-2)	2.1978e-1 (3.01e-2)
mDTLZ4	5	3.5856e-1 - (1.85e-2)	3.3311e-1 - (1.38e-1)	3.8760e-1 - (1.96e-1)	**3.0939e-1** (2.05e-1)
+/-/=		0/8/0	0/8/0	1/6/1	–

Table 5. Means and standard deviations of HV metric values obtained by MOEA/D-SPP and its variants.

HV	m	V-a	V-b	V-c	MOEA/D-SPP
mDTLZ1	3	4.1774e-1 - (1.54e-2)	5.0819e-1 - (1.65e-3)	2.8524e-1 - (7.52e-2)	**5.2067e-1** (3.01e-2)
mDTLZ2	3	1.0157e+0 - (1.51e-3)	1.0089e+0 - (3.93e-3)	9.6192e-1 - (6.11e-3)	**1.0340e+0** (1.16e-3)
mDTLZ3	3	1.0143e+0 - (3.27e-3)	1.0001e+0 - (4.86e-3)	9.0952e-1 - (1.02e-1)	**1.0314e+0** (4.75e-3)
mDTLZ4	3	7.2188e-1 - (2.49e-1)	8.5774e-1 = (2.18e-1)	6.6940e-1 - (2.02e-1)	**8.8277e-1** (1.83e-1)
mDTLZ1	5	4.6000e-2 - (7.03e-5)	7.0221e-2 - (2.16e-3)	3.1131e-2 - (3.29e-3)	**7.7432e-2** (6.42e-3)
mDTLZ2	5	2.9611e-1 - (2.94e-3)	4.0922e-1 - (4.33e-3)	4.3055e-1 - (3.80e-3)	**4.6319e-1** (2.30e-3)
mDTLZ3	5	3.3234e-1 - (4.40e-3)	4.0958e-1 - (5.13e-3)	3.0990e-1 - (1.18e-2)	**4.6964e-1** (3.11e-3)
mDTLZ4	5	2.3319e-1 - (5.87e-2)	3.0144e-1 = (1.03e-1)	1.3606e-1 - (1.10e-1)	**3.0900e-1** (1.30e-1)
+/-/=		0/8/0	0/6/2	0/8/0	–

Table 6. Average ranks of MOEA/D-SPP and its variants obtained by Friedman test

	IGD	HV
V-a	3	2.875
V-b	2.875	2.375
V-c	2.875	3.75
MOEA/D-SPP	**1.25**	**1**

both IGD and HV metrics across most instances. According to Table 6, V-a

demonstrates competitive overall performance compared to V-b and V-c. On the one hand, **IdentifyDRS** eliminates DRSs and fosters population convergence. Thus it may make the population lack diversity in V-b. On the other hand, **AdjustWeights** estimates the PF shape using the population with DRSs in V-c, making the estimation highly inaccurate. Therefore, MOEA/D-SPP simultaneously employs the two strategies, striking a better balance between convergence and diversity and having the best performance.

5 Conclusion

In this study, we have introduced the PPO metric and proposed MOEA/D-SPP. The PPO metric aims to identify DRSs, while MOEA/D-SPP implements it to alleviate the adverse effects of DRSs. **AdjustWeights**, namely the one-shot weight vector adjustment in MOEA/D-SPP, further enhances the population diversity. To comprehensively assess the efficacy of the proposed algorithm, we have conducted experimental evaluations on benchmarks of DRS-MOPs, specifically 3-objective and 5-objective mDTLZ1-mDTLZ4. The performance of MOEA/D-SPP is compared against five representative MOEAs. The obtained results reveal the promising performance of MOEA/D-SPP in addressing DRS-MOPs. Additionally, ablation experiments have validated the effectiveness of each algorithmic component in MOEA/D-SPP.

In the future, we plan to extend the applicability of the PPO metric to other categories of MOEAs (i.e., dominance-based MOEAs and indicator-based MOEAs), aiming to enhance their performance in addressing DRS-MOPs. We also intend to delve into real-world scenarios involving DRSs and apply our algorithm.

Acknowledgments. This work was supported by the National Natural Science Foundation of China (Grant No. 62106096), the Natural Science Foundation of Guangdong Province (Grant No. 2024A1515011759), the National Natural Science Foundation of Shenzhen (Grant No. JCYJ20220530113013031), and the 2023 Graduate Innovation Practice Fund Project of Southern University of Science and Technology.

References

1. Bader, J., Zitzler, E.: HypE: An algorithm for fast hypervolume-based many-objective optimization. Evolutionary Computation **19**(1), 45–76 (2011)
2. Batista, L.S., Campelo, F., Guimarães, F.G., Ramírez, J.A.: A comparison of dominance criteria in many-objective optimization problems. In: 2011 IEEE Congress of Evolutionary Computation (CEC). pp. 2359–2366. IEEE (2011)
3. Bellman, R.: Dynamic programming. Princeton University Press, Princeton, NJ, USA **1**, 3–25 (1958)
4. Coello, C.A.C., Cortés, N.C.: Solving multiobjective optimization problems using an artificial immune system. Genetic Programming and Evolvable Machines **6**, 163–190 (2005)

5. Deb, K., Goyal, M., et al.: A combined genetic adaptive search (GeneAS) for engineering design. Computer Science and Informatics **26**, 30–45 (1996)
6. Deb, K., Jain, H.: An evolutionary many-objective optimization algorithm using reference-point-based nondominated sorting approach, part I: solving problems with box constraints. IEEE Transactions on Evolutionary Computation **18**(4), 577–601 (2013)
7. Deb, K., Mohan, M., Mishra, S.: Towards a quick computation of well-spread Pareto-optimal solutions. In: Evolutionary Multi-Criterion Optimization: Second International Conference, EMO 2003, Faro, Portugal, April 8–11, 2003. Proceedings 2. pp. 222–236. Springer (2003)
8. Deb, K., Pratap, A., Agarwal, S., Meyarivan, T.: A fast and elitist multiobjective genetic algorithm: NSGA-II. IEEE Transactions on Evolutionary Computation **6**(2), 182–197 (2002)
9. Deb, K., do Val Lopes, C.L., Martins, F.V.C., Wanner, E.F.: Identifying Pareto fronts reliably using a multi-stage reference-vector-based framework. IEEE Transactions on Evolutionary Computation **28**(1), 252–266 (2024)
10. Di Pierro, F., Khu, S.T., Savic, D.A.: An investigation on preference order ranking scheme for multiobjective evolutionary optimization. IEEE Transactions on Evolutionary Computation **11**(1), 17–45 (2007)
11. Duan, J., He, Z., Yen, G.G.: Robust multiobjective optimization for vehicle routing problem with time windows. IEEE Transactions on Cybernetics **52**(8), 8300–8314 (2021)
12. Emmerich, M., Beume, N., Naujoks, B.: An EMO algorithm using the hypervolume measure as selection criterion. In: International Conference on Evolutionary Multi-Criterion Optimization. pp. 62–76. Springer (2005)
13. Geoffrion, A.M.: Proper efficiency and the theory of vector maximization. Journal of Mathematical Analysis and Applications **22**(3), 618–630 (1968)
14. Giagkiozis, I., Fleming, P.J.: Methods for multi-objective optimization: An analysis. Information Sciences **293**, 338–350 (2015)
15. Giagkiozis, I., Purshouse, R.C., Fleming, P.J.: Generalized decomposition. In: International Conference on Evolutionary Multi-Criterion Optimization. pp. 428–442. Springer (2013)
16. Guerreiro, A.P., Fonseca, C.M.: Hypervolume sharpe-ratio indicator: Formalization and first theoretical results. In: Parallel Problem Solving from Nature–PPSN XIV: 14th International Conference, Edinburgh, UK, September 17-21, 2016, Proceedings 14. pp. 814–823. Springer (2016)
17. Hastie, T., Tibshirani, R., Friedman, J.H., Friedman, J.H.: The elements of statistical learning: data mining, inference, and prediction, vol. 2. Springer (2009)
18. Ikeda, K., Kita, H., Kobayashi, S.: Failure of Pareto-based MOEAs: Does non-dominated really mean near to optimal? In: Proceedings of the 2001 Congress on Evolutionary Computation (IEEE Cat. No. 01TH8546). vol. 2, pp. 957–962. IEEE (2001)
19. Ishibuchi, H., Akedo, N., Nojima, Y.: A study on the specification of a scalarizing function in MOEA/D for many-objective knapsack problems. In: International Conference on Learning and Intelligent Optimization (LION). pp. 231–246. Springer (2013)
20. Ishibuchi, H., Setoguchi, Y., Masuda, H., Nojima, Y.: Performance of decomposition-based many-objective algorithms strongly depends on Pareto front shapes. IEEE Transactions on Evolutionary Computation **21**(2), 169–190 (2016)

21. Li, K., Wang, H., Wang, W., Wang, F., Cui, Z.: Improving artificial bee colony algorithm using modified nearest neighbor sequence. Journal of King Saud University-Computer and Information Sciences **34**(10), 8807–8824 (2022)
22. Li, K., Xu, M., Zeng, T., Ye, T., Zhang, L., Wang, W., Wang, H.: A new artificial bee colony algorithm based on modified search strategy. International Journal of Computing Science and Mathematics **15**(4), 387–395 (2022)
23. Li, K., Deb, K., Zhang, Q., Kwong, S.: An evolutionary many-objective optimization algorithm based on dominance and decomposition. IEEE Transactions on Evolutionary Computation **19**(5), 694–716 (2014)
24. Liang, Z., Hu, K., Ma, X., Zhu, Z.: A many-objective evolutionary algorithm based on a two-round selection strategy. IEEE Transactions on Cybernetics **51**(3), 1417–1429 (2019)
25. Liu, H.l., Li, X.: The multiobjective evolutionary algorithm based on determined weight and sub-regional search. In: 2009 IEEE Congress on Evolutionary Computation (CEC). pp. 1928–1934. IEEE (2009)
26. Liu, Y., Liu, J., Teng, X.: Single-particle optimization for network embedding preserving both local and global information. Swarm and Evolutionary Computation **71**, 101069 (2022)
27. Liu, Y., Liu, J., Wu, K.: Cost-effective competition on social networks: A multi-objective optimization perspective. Information Sciences **620**, 31–46 (2023)
28. Liu, Y., Zhu, N., Li, M.: Solving many-objective optimization problems by a Pareto-based evolutionary algorithm with preprocessing and a penalty mechanism. IEEE Transactions on Cybernetics **51**(11), 5585–5594 (2020)
29. López Jaimes, A., Coello Coello, C.A., Aguirre, H., Tanaka, K.: Adaptive objective space partitioning using conflict information for many-objective optimization. In: Evolutionary Multi-Criterion Optimization: 6th International Conference, EMO 2011, Ouro Preto, Brazil, April 5-8, 2011. Proceedings 6. pp. 151–165. Springer (2011)
30. Miettinen, K.: Nonlinear multiobjective optimization, vol. 12. Springer Science & Business Media (2012)
31. Pang, L.M., Ishibuchi, H., Shang, K.: NSGA-II with simple modification works well on a wide variety of many-objective problems. IEEE Access **8**, 190240–190250 (2020)
32. Tian, Y., Cheng, R., Zhang, X., Jin, Y.: PlatEMO: A MATLAB platform for evolutionary multi-objective optimization [educational forum]. IEEE Computational Intelligence Magazine **12**(4), 73–87 (2017)
33. Wang, Z., Li, Q., Li, G., Zhang, Q.: Multi-objective decomposition evolutionary algorithm with objective modification-based dominance and external archive. Applied Soft Computing **149**, 111006 (2023)
34. Wang, Z., Li, Q., Yang, Q., Ishibuchi, H.: The dilemma between eliminating dominance-resistant solutions and preserving boundary solutions of extremely convex Pareto fronts. Complex & Intelligent Systems **9**(2), 1117–1126 (2023)
35. Wang, Z., Ong, Y.S., Ishibuchi, H.: On scalable multiobjective test problems with hardly dominated boundaries. IEEE Transactions on Evolutionary Computation **23**(2), 217–231 (2018)
36. Wang, Z., Yao, S., Li, G., Zhang, Q.: Multiobjective combinatorial optimization using a single deep reinforcement learning model. IEEE Transactions on Cybernetics **54**(3), 1984–1996 (2024)
37. Wang, Z., Zhang, Q., Zhou, A., Gong, M., Jiao, L.: Adaptive replacement strategies for MOEA/D. IEEE Transactions on Cybernetics **46**(2), 474–486 (2015)

38. Wang, Z., Zhen, H.L., Deng, J., Zhang, Q., Li, X., Yuan, M., Zeng, J.: Multiobjective optimization-aided decision-making system for large-scale manufacturing planning. IEEE Transactions on Cybernetics **52**(8), 8326–8339 (2021)
39. Wei, Z., Wang, H., Wang, S., Zhang, S., Xiao, D.: Complementary environmental selection for evolutionary many-objective optimization. In: International Conference on Neural Computing for Advanced Applications. pp. 346–359. Springer (2023)
40. Wei, Z., Wang, H., Wang, S., Zhang, Z., Cui, Z., Wang, F., Peng, H., Zhao, J.: Many-objective evolutionary algorithm based on parallel distance for handling irregular pareto fronts. Swarm and Evolutionary Computation **86**, 101539 (2024)
41. Ye, R., Chen, L., Liao, W., Zhang, J., Ishibuchi, H.: Data-Driven Preference Sampling for Pareto Front Learning. arXiv preprint arXiv:2404.08397 (2024)
42. Ye, R., Chen, L., Zhang, J., Ishibuchi, H.: Evolutionary Preference Sampling for Pareto Set Learning. arXiv preprint arXiv:2404.08414 (2024)
43. Ye, R., Tang, M.: PraFFL: A Preference-Aware Scheme in Fair Federated Learning. arXiv preprint arXiv:2404.08973 (2024)
44. Yuan, Y., Xu, H., Wang, B., Yao, X.: A new dominance relation-based evolutionary algorithm for many-objective optimization. IEEE Transactions on Evolutionary Computation **20**(1), 16–37 (2015)
45. Zhang, Q., Li, H.: MOEA/D: A multiobjective evolutionary algorithm based on decomposition. IEEE Transactions on Evolutionary Computation **11**(6), 712–731 (2007)
46. Zheng, R., Wang, Z.: A generalized scalarization method for evolutionary multiobjective optimization. In: Proceedings of the AAAI Conference on Artificial Intelligence (AAAI). vol. 37, pp. 12518–12525 (2023)
47. Zitzler, E., Thiele, L.: Multiobjective evolutionary algorithms: A comparative case study and the strength Pareto approach. IEEE Transactions on Evolutionary Computation **3**(4), 257–271 (1999)